Inclusive photoproduction of bottom quarks for low and medium p_T in the general-mass variable-flavour-number scheme

G. Kramer [a], H. Spiesberger [b,c,*]

[a] *II. Institut für Theoretische Physik, Universität Hamburg, Luruper Chaussee 149, D-22761 Hamburg, Germany*
[b] *PRISMA Cluster of Excellence, Institut für Physik, Johannes Gutenberg-Universität, 55099 Mainz, Germany*
[c] *Centre for Theoretical and Mathematical Physics and Department of Physics, University of Cape Town, Rondebosch 7700, South Africa*

A B S T R A C T

We present predictions for b-quark production in photoproduction and compare with experimental data from HERA. Our theoretical predictions are obtained at next-to-leading-order in the general-mass variable-flavor-number scheme, an approach which takes into account the finite mass of the b quarks. We use realistic evolved nonperturbative fragmentation functions obtained from fits to e^+e^- data. We find in general good agreement of data with both the GM-VFNS and the FFNS calculations, while the more precise ZEUS data seem to prefer the GM-VFNS predictions.

1. Introduction

The investigation of heavy-quark (bottom or charm) production in ep collisions is a useful test of perturbative Quantum Chromodynamics (QCD) since the heavy quark mass provides a hard scale that allows to perform calculations within perturbation theory. At leading order (LO), boson–gluon fusion, $\gamma g \to b\bar{b}$ is the dominant process for bottom-quark production. When the negative squared four-momentum of the initial and final electron, Q^2, is small, the process $ep \to ebX$ is treated as photoproduction, in which a quasi-real photon emitted by the initial electron interacts with the partons in the proton (direct contribution). For $Q^2 \simeq 0$, in addition to the direct contributions, there are also resolved contributions, where the incoming photon changes into an initial quark or gluon, which interact with partons from the incoming proton.

Bottom photoproduction has been measured using several different methods by the H1 [2] and ZEUS [3] Collaborations at HERA. In most of the measurements, the cross section was obtained using semi-leptonic decays into muons or electrons. All these measurements have been compared with predictions based on the fixed-flavor-number scheme (FFNS) [1]. In this scheme, the bottom quark is generated in the hard scattering-process and appears only in the final state. Predictions for the photoproduction cross section are calculated at next-to-leading-order (NLO) taking the finite mass of

the bottom quark explicitly into account. Reasonable agreement of the data with FFNS predictions has been obtained.

In the large-p_T region, characterized by $p_T \gg m_b$, the so-called massless or zero-mass variable flavor-number-scheme (ZM-VFNS) [4–6] is considered more appropriate. This is the conventional parton model approach, where the b quark, considered massless like any other incoming parton, is also an incoming parton from the proton and, for the resolved contribution, from the incoming photon. This gives rise to additional contributions from hard-scattering subprocesses with b quarks in the initial state, besides those with u, d, s and c quarks and the gluon (g). Predictions in this approach are reliable only in the large p_T-region where terms of the order m_b^2/p_T^2 are negligible. Calculations at NLO automatically resum leading and next-to-leading logarithmic terms $\propto \ln(p_T^2/m_b^2)$. At the same time, all non-logarithmic terms through $O(\alpha_s^2)$ are retained for $m_b = 0$. With the usual choice of renormalization (μ_R) and factorization scales (μ_I and μ_F for initial and final-state factorization, resp.), $\mu_R = \mu_I = \mu_F = m_T = \sqrt{p_T^2 + m_b^2}$, the results are dominated by contributions from the b-quark PDF of the proton down to $p_T = 0$.

The neglect of the terms of order m_b^2/p_T^2 in the hard scattering cross section is remedied in the general-mass variable-flavor-number scheme (GM-VFNS) [7]. This theoretical framework combines the FFN and the ZM-VFN schemes. The mass-dependent terms of the FFNS are added to the ZM-VFNS by applying subtractions in such a way that in the limit $p_T \to \infty$ the hard-scattering cross sections in the ZM-VFNS are recovered. However, with the conventional choice of scales indicated above, the results in the

* Corresponding author at: PRISMA Cluster of Excellence, Institut für Physik, Johannes Gutenberg-Universität, 55099 Mainz, Germany.
E-mail address: spiesber@uni-mainz.de (H. Spiesberger).

GM-VFNS are still dominated by the contributions of the b-quark PDF down to $p_T \simeq 0$. Therefore, there is no smooth transition from the GM-VFNS at large p_T values to the FFNS in the small-p_T range, and the GM-VFNS in its original definition fails to describe the small-p_T cross sections.

The dominance of contributions with b-quarks in the initial state at small p_T-values is connected to the fact that this part is treated in the massless scheme. A calculation of the b-quark initiated subprocesses in a scheme with massive partons is not available for photo- and for hadroproduction.[1] In addition it would be necessary to correctly describe the effects of the finite bottom-quark mass m_b in the DGLAP evolution. Attempts in this direction have been presented in [9].

The cross section with massless partons is divergent for $p_T \to 0$. For a realistic description it is therefore necessary to eliminate the contribution with massless b-quarks in the initial state in the small-p_T region. For inclusive B-meson production in pp ($p\bar{p}$) collisions this has been achieved in recent work together with Kniehl and Schienbein [10] by a suitable choice of scales μ_I and μ_F. In this modified GM-VFNS the FFNS results with the exact m_b dependence are recovered at small p_T. This way reasonable results were obtained for the inclusive B-meson production cross section measured with CDF at the Fermilab Tevatron and with LHCb at the CERN LHC.

It is the aim of this work to apply the same prescription for the choice of the factorization scales to b-quark photoproduction. For the resolved part the modified prescription works as described in [10] for hadron–hadron scattering. For the direct part a corresponding calculation has not been done yet. We shall do this here and compare our results to recent ZEUS and H1 cross section data in order to study whether the modifications of the GM-VFNS can lead to a better agreement with presently available experimental data.

Cross sections for inclusive charmed-hadron photoproduction have been calculated in the past [11,12], but without the scale modifications described in [10]. The corresponding experimental data are not available for very small p_T, where the modifications would be most clearly visible. For somewhat larger p_T, very good agreement of the various observables for inclusive D^* photoproduction has been found [13].

The outline of this paper is as follows. In Sect. 2 we introduce our strategy for the transition to the FFNS and compare our predictions with the ZEUS and H1 data. Our conclusions are presented in Sect. 3.

2. Results and comparison with ZEUS and H1 data

In this section, we shall consider a viable framework for inclusive h_b production, where h_b is any hadron containing a b-quark. Our aim is to unify prescriptions for the calculation of theoretical predictions at small and at large p_T-values. We shall compare with the differential cross section $d\sigma/dp_T$ measured by the ZEUS and the H1 Collaborations at HERA. We take the b-quark pole mass to be $m_b = 4.5$ GeV, evaluate $\alpha_s^{(n_f)}(\mu_R)$ at NLO with $n_f = 4$ and $\Lambda_{\overline{MS}}^{(4)} = 328$ MeV if $\mu_R < m_b$ and with $n_f = 5$ and $\Lambda_{\overline{MS}}^{(5)} = 226$ MeV if $\mu_R > m_b$. For the proton PDFs we use the parametrization CTEQ6.6 [14] while for the photon PDF we use AFG04_BF [15] as our default, but we will also consider other PDF choices for comparison.

We start with results to be compared with the ZEUS data [3] shown in Fig. 1 together with our theoretical predictions. The

data have been measured in various different analysis. Only five data points were reported in [3]. The other 13 points are from earlier publications. Their origin can be traced back from Fig. 8 of [3]. The ZEUS data are for the differential cross section for b-quark production as a function of p_T (between 5 and 30 GeV) with the kinematic constraints $Q^2 < 1$ GeV^2 for the momentum transfer squared, $0.2 < y < 0.8$ for the inelasticity $y = Q^2/(x_{Bj}S)$ (where x_{Bj} is the Bjorken scaling variable and S the total energy in the center-of-mass reference frame) and $|y_b| < 2.0$ for the b-quark pseudo-rapidity. The data points at $p_T = 9.25, 12.5, 17.5, 22.5, 28.75$ GeV from [3] have in average smaller experimental errors than the earlier measurements since they are measured with the largest integrated luminosity of 133 pb^{-1}. Note that not all points are consistent with each other, i.e. for some points the systematic errors are presumably larger than given in [3]. In most of the previous measurements of bottom photoproduction at HERA, the cross section was determined using semi-leptonic decays into muons or electrons. In [3] the b-quark photoproduction cross sections were determined for the production of jets containing b-quarks. The cross sections for the production of b-jets have been converted into cross sections for b-quark production with the help of the FMNR program [18]. In Fig. 8 of Ref. [3] the data have been compared with predictions of the FFNS [1].

In Fig. 1 (upper left frame), we compare the ZEUS data with NLO predictions in the GM-VFNS. Our framework has been described in detail in Refs. [11,12] for photoproduction of D^* mesons. The full line in Fig. 1 (upper left frame) shows the result for the old default choice of scales, $\mu_i = \xi_i m_T$ with $\xi_i = 1$ for $i = R, I, F$ where R, I, and F denote renormalization, initial-state and final-state factorization scales. The dashed lines represent an estimate of the theoretical error by varying ξ_i up and down by a factor of 2. 13 data points agree with the theoretical prediction within experimental and theoretical errors, 5 points lie outside this range.

The central curve in Fig. 1 (upper left frame), as well as the curve for the upper error estimate, show the characteristic behaviour of a monotonic increase of $d\sigma/dp_T$ in the limit $p_T \to 0$. This behaviour is caused by the scale choice with $\xi_I \geq 1$. The curve for the lower error estimate with $\xi_I = 0.5$, however, shows a turn-over towards small p_T with a maximum at $p_T \simeq 3$ GeV. This is the same characteristic behaviour as in the FFNS [2,3] and is caused in our case by the fact that at around $p_T = 7.7$ GeV the factorization scales $\mu_i = \xi_i m_T = m_T/2$ fall below m_b where the b-quark PDF and FF are zero. The same typical turn-over was also found in our previous study of inclusive B-meson production for pp and $p\bar{p}$ collisions [10].

Actually, the b-quark cross section is calculated from the B-meson cross section using an evolved fragmentation function (FF) for $b \to B$ taken from [19] and dividing by the branching fraction $Br(b \to B) = 0.40$. The effect of the evolved FF is visible at larger values of $p_T > 20$ GeV where the cross section $d\sigma/dp_T$ is smaller than without a FF. We emphasize that a consistent theoretical prescription of the GM-VFNS requires to include a FF describing the $b \to h_b$ transition since final state singularities have to be subtracted from the bare cross section in analogy to the calculation in the ZM-VFNS.

Unfortunately all the ZEUS measurements are for $p_T \geq 5$ GeV, so that any turn-over of the cross section $d\sigma/dp_T$ towards $p_T = 0$ is not measured. All data points agree reasonably well also with the GM-VFNS predictions with the original default scale $\mu_R = \mu_I = \mu_F = m_T$.

A monotonic increase of the cross section $d\sigma/dp_T$ for the production of a massive quark towards small p_T is unphysical. From our previous work on B-meson production in pp and $p\bar{p}$ collisions [10] we know how the choice of the factorization scales must

---

[1] For deep inelastic scattering heavy-quark initiated processes at NLO with massive quarks have been considered in Ref. [8].
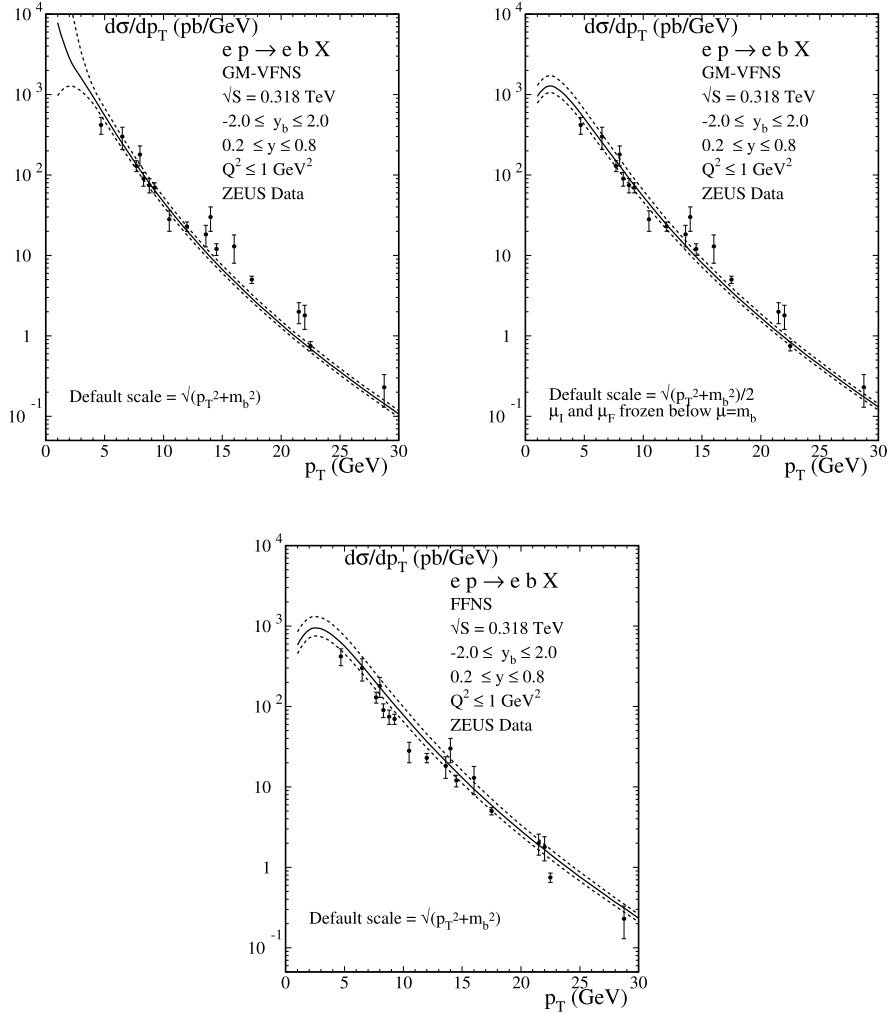
Fig. 1. Differential cross section $d\sigma/dp_T$ for bottom-quark production as a function of the transverse momentum p_T of the bottom quark compared with ZEUS data [3]. The upper left frame is for the original GM-VFNS choice of default scales $\mu_R = \mu_I = \mu_F = m_T$; the upper right frame shows results with the new default scale $\mu_R = m_T$, $\mu_I = \mu_F = m_T/2$. For comparison we also show in the lower panel results of the FFNS with $\mu_R = \mu_I = m_T$ (no FF).

be modified in order to obtain cross sections for $p_T \to 0$ which show the expected behaviour. Therefore, as in [10], we choose as the new default scales $\mu_R = m_T$ and $\mu_I = \mu_F = m_T/2$ such that both the b-quark PDF and the FF for the $b \to h_b$ transition vanish for $\mu_F < m_b$ already at non-zero p_T. With $\xi_R = 1$, $\xi_I = \xi_F = 0.5$ as the new default scale choice, we estimate the theoretical error in the usual way by varying the renormalization scale parameter μ_R by a factor 2 up and down about the default scale. We have not introduced an extra prescription to freeze μ_R below m_b because the choice of μ_R is not related to switching off b-quark initiated subprocesses. The resulting error band is shown in Fig. 1 (upper right frame) together with the full curve for the new default choice and the ZEUS data [3]. The agreement with the data is only marginally better than in the upper left frame of Fig. 1. Since the data have p_T values larger than 5 GeV the turn-over of $d\sigma/dp_T$ towards $p_T \to 0$ is not tested by the ZEUS measurements.

In the lower part of Fig. 1 we compare the ZEUS data with results obtained in the FFNS. Here we have fixed the scales to $\mu_R = \mu_I = m_T$. The FFNS prediction is only slightly below the GM-VFNS calculation at low p_T, but lies above it by about a factor of two at the largest p_T. The difference at large p_T is mainly due to the fact that the FFNS calculation does not include an evolved FF. We observe that the FFNS calculation over-shoot the high-precision data points of ZEUS.

Similar data are available from the H1 Collaboration at HERA. The most recent publication [2] describes results for photoproduction of b-quarks measured in the process $ep \to eb\bar{b}X$. The decay channel $b\bar{b} \to eeX$ is selected by identifying the semi-electronic decays of the b-quarks. The production cross section is measured in the kinematic range where the photon virtuality is small, $Q^2 \leq 1$ GeV^2, the inelasticity is restricted to the range $0.05 \leq y \leq 0.65$ and the pseudorapidity of the b-quarks is in the range $|y_b| \leq 2$. The measured cross sections are converted into single-inclusive b-quark production cross sections $d\sigma/dp_T$ for four p_T bins in the range $0 \leq p_T \leq 30$ GeV. We have calculated the $ep \to ebX$ cross section $d\sigma/dp_T$ as a function of p_T in this p_T range and with the same kinematic constraints as in [2] in the original GM-VFNS with default scales $\xi_R = \xi_I = \xi_F = 1$ and with the new default scales $\xi_R = 1$, $\xi_I = \xi_F = 0.5$. The results, together with scale variations as above to obtain an error estimate, are shown in Fig. 2 together with the H1 data. The upper left panel of Fig. 2 shows results for the original scale setting, the upper right frame is for the new scale choice. The experimental data for $p_T > 5$ GeV agree with the predictions in both schemes. Only the cross section $d\sigma/dp_T$ in the lowest-p_T bin, $0 \leq p_T \leq 4.65$ GeV, is lower than the predictions in both cases. In this p_T-bin the measured cross section is smaller than the theory prediction by approximately a factor of 6 in the upper left frame of Fig. 2 and by a factor 3 to 4 in the
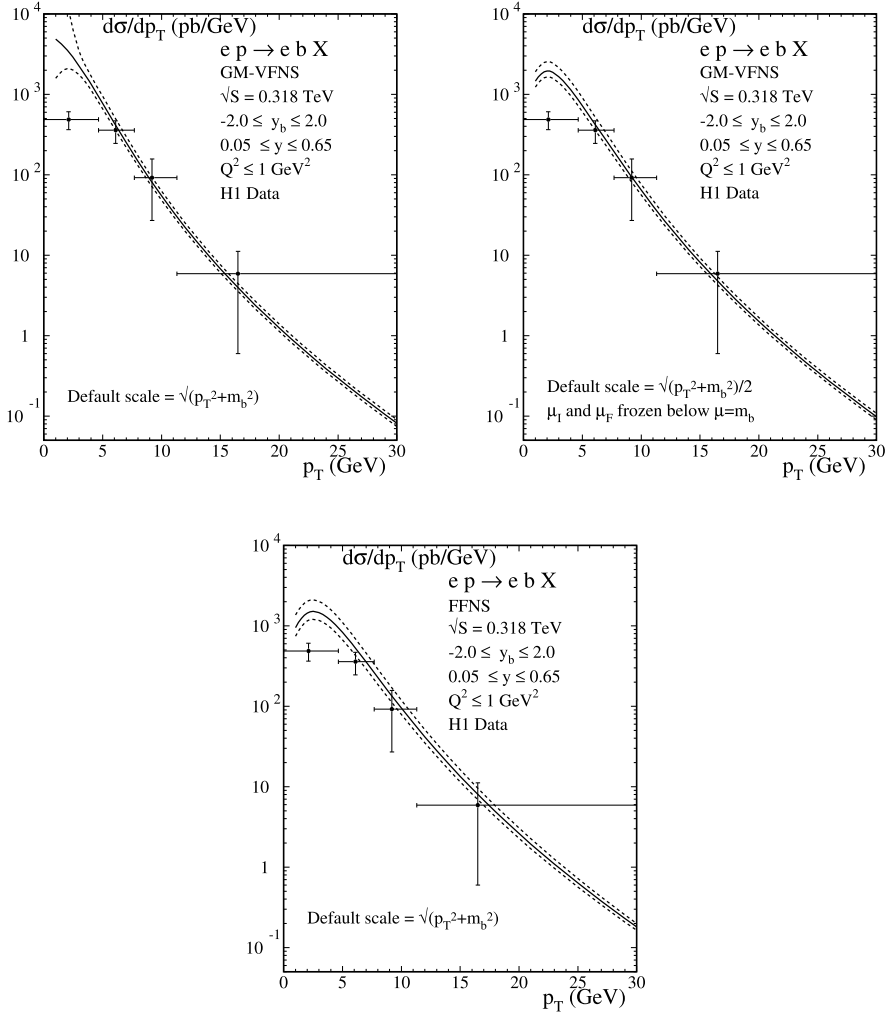
Fig. 2. Differential cross section $d\sigma/dp_T$ for bottom photoproduction as a function of the transverse momentum p_T compared to H1 data [2]. The upper left frame is for the original GM-VFNS choice of scale parameters $\mu_R = \mu_I = \mu_F = m_T$ and the upper right frame for the new default scales $\mu_R = m_T$, $\mu_I = \mu_F = m_T/2$. FFNS results with $\mu_R = \mu_I = m_T$ (no FF) are shown in the lower frame.

upper right frame of Fig. 2. Although the p_T-dependence of the differential cross section $d\sigma/dp_T$ exhibits the expected turn-over at $p_T \simeq 2$ GeV if the new default scales are chosen, the predicted cross section is still larger than the experimental data, even when taking into account the experimental uncertainty.

A comparison of the data with the FFNS prediction is shown in the lower frame of Fig. 2, again choosing scales as $\mu_R = \mu_I = m_T$ and without folding with a FF. As above, the FFNS results are slightly below those of the GM-VFNS at low p_T, but above at large p_T. We note that the NLO corrections in the FFNS are positive and lead to an increase of the cross section by about a factor of 1.5 at low p_T. The H1 data with its relatively large errors are unable to discriminate between the two schemes. We should remark that the H1 data are presented as a function of the average transverse momentum of two produced bottom quarks, while our calculation is for the one-particle inclusive cross section where the independent kinematic variable is the transverse momentum of one observed b-quark. This may be the reason that the theoretical predictions shown in [2] do not agree with our FFNS evaluation.

In order to study the influence of the choice of the proton PDF we present also results for two other PDFs: CT10 [20] and HERA-PDF1.5 (NLO) [21]. The results are shown in Fig. 3 (left frame) as ratios to the prediction obtained for the default choice CTEQ6.6.

The differences to CTEQ6.6 are very small, in particular for CT10, as to be expected. For HERAPDF1.5 the difference is somewhat larger. In the range $2 < p_T < 20$ GeV the cross section with HER-APDF1.5 is larger than for CTEQ6.6 and for larger p_T values, $p_T > 20$ GeV, the ratio is smaller than 1 and decreases towards 0.9 for $p_T = 30$ GeV.

We include also a comparison with two different choices of the photon PDFs, shown in the right frame of Fig. 3. Again, we present the results as a ratio of cross sections and choose the GRV HO [16,17] photon PDF as an alternative to the AFG04 parametrization. The cross section ratio is very close to 1. Only for the smallest considered p_T value the ratio reaches values slightly above 1.06.

As is well-known, a complete calculation of the photoproduction cross section has to take into account two parts, the direct contribution and the resolved contribution. It is interesting to study whether both parts show the same dependence on p_T. To see this in some detail we have calculated these two parts separately, denoted $d\sigma^{dir}/dp_T$ and $d\sigma^{res}/dp_T$. Results for the H1 kinematic conditions are shown in Fig. 4. For the sake of a more clear visibility we display the ratios of $d\sigma^x/dp_T$ and $d\sigma^{tot}/dp_T$ where $x = $ dir, res and $d\sigma^{tot}/dp_T = d\sigma^{dir}/dp_T + d\sigma^{res}/dp_T$ is the sum of the direct and resolved contributions as shown Fig. 2 (upper right frame). From Fig. 4 we see that the resolved cross section
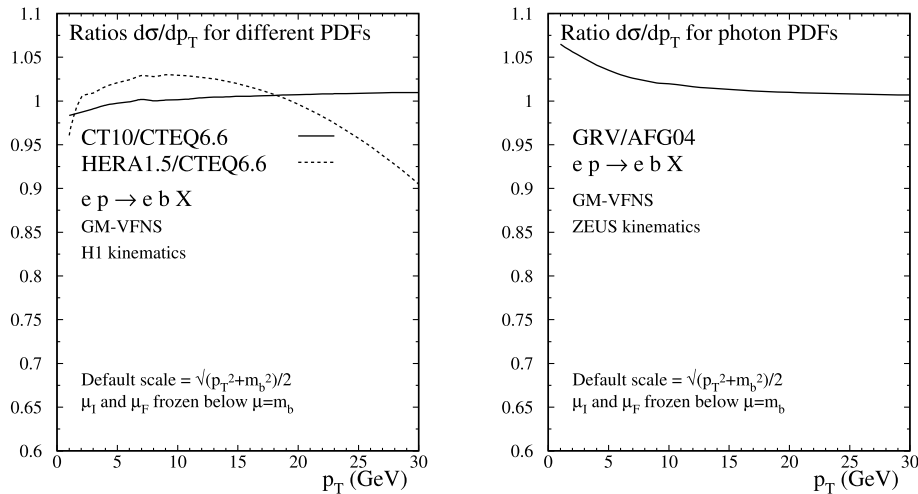
Fig. 3. Left frame: ratios of the differential cross sections $d\sigma/dp_T$ for bottom photoproduction using different proton PDF parametrizations with respect to the default CTEQ6.6 [14] PDF. The full curve is for CT10 [20], the dashed curve for HERAPDF1.5 [21]. Right frame: ratio of the differential cross section $d\sigma/dp_T$ for bottom photoproduction as a function the transverse momentum p_T for the photon PDF GRV HO [16,17] with respect to the photon PDF AFG04 [15]. In both figures, the kinematic constraints of the ZEUS data and the new default scales $\mu_R = m_T$, $\mu_I = \mu_F = m_T/2$ have been used.
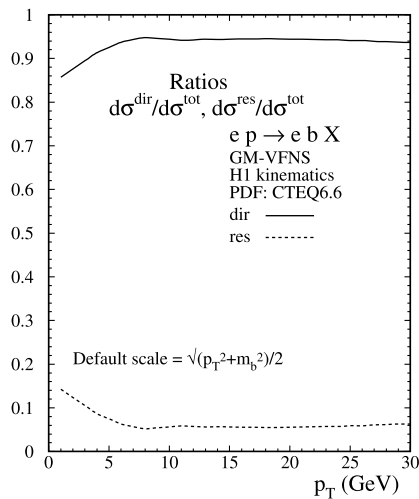

Fig. 4. Ratios of $d\sigma^{\mathrm{dir}}/dp_T$ and $d\sigma^{\mathrm{res}}/dp_T$ to the total cross section $d\sigma^{\mathrm{tot}}/dp_T$ as a function of the transverse momentum p_T of the b-quark.

varies between 6% and 15% for $p_T < 5$ GeV, while it stays near 6% for the larger p_T values. This means that even when the resolved part would vanish for all p_T the direct part would change by less than 15%. This is too small to be identified unambiguously in the data. In particular, a different p_T dependence of the direct part cannot be made responsible for the low cross section measured by H1 at $p_T = 2$ GeV.

3. Conclusions

We have presented predictions for b-quark photoproduction at HERA at next-to-leading order in the general-mass variable-flavor-number scheme. In contrast to previous calculations, we have fixed the factorization scale parameters in such a way that b-quark initiated contributions are eliminated at low transverse momenta. With this new prescription we recover the typical low-p_T behaviour of a fixed-flavor-number scheme. The comparison with

experimental data from the ZEUS Collaboration shows reasonable agreement over the whole range of transverse momenta, while we observe a discrepancy in the lowest-p_T bin of the H1 measurement.

References

[1] S. Frixione, P. Nason, G. Ridolfi, Nucl. Phys. B 454 (1995) 3, arXiv:hep-ph/9506226.
[2] F.D. Aaron, et al., H1 Collaboration, Eur. Phys. J. C 72 (2012) 2148, arXiv:1206.4346 [hep-ex], and earlier references found there.
[3] H. Abramowicz, et al., ZEUS Collaboration, Eur. Phys. J. C 71 (2011) 1659, arXiv:1104.5444 [hep-ex], and earlier references found there.
[4] M. Cacciari, M. Greco, Nucl. Phys. B 421 (1994) 530, arXiv:hep-ph/9311260.
[5] B.A. Kniehl, M. Krämer, G. Kramer, M. Spira, Phys. Lett. B 356 (1995) 539, arXiv:hep-ph/9505410.
[6] M. Cacciari, M. Greco, B.A. Kniehl, M. Krämer, G. Kramer, M. Spira, Nucl. Phys. B 466 (1996) 173, arXiv:hep-ph/9512246.
[7] B.A. Kniehl, G. Kramer, I. Schienbein, H. Spiesberger, Phys. Rev. D 79 (2009) 094009, arXiv:0901.4130 [hep-ph], and earlier work quoted there.
[8] S. Kretzer, I. Schienbein, Phys. Rev. D 58 (1998) 094035, arXiv:hep-ph/9805233.
[9] E.G. de Oliveira, A.D. Martin, M.G. Ryskin, A.G. Shuvaev, Eur. Phys. J. C 73 (2013) 2616, arXiv:1307.3508 [hep-ph].
[10] B.A. Kniehl, G. Kramer, I. Schienbein, H. Spiesberger, Eur. Phys. J. C 75 (2015) 140, arXiv:1502.01001 [hep-ph].
[11] G. Kramer, H. Spiesberger, Eur. Phys. J. C 38 (2004) 309, arXiv:hep-ph/0311062.
[12] B.A. Kniehl, G. Kramer, I. Schienbein, H. Spiesberger, Eur. Phys. J. C 62 (2009) 365, arXiv:0902.3166 [hep-ph].
[13] F.D. Aaron, et al., H1 Collaboration, Eur. Phys. J. C 72 (2012) 1995, arXiv:1203.1170 [hep-ex].
[14] P.M. Nadolsky, et al., CTEQ Collaboration, Phys. Rev. D 78 (2008) 013004, arXiv:0802.0007 [hep-ph].
[15] P. Aurenche, M. Fontannaz, J.P. Guillet, Eur. Phys. J. C 44 (2005) 395, arXiv:hep-ph/0503259.
[16] M. Glück, E. Reya, A. Vogt, Phys. Rev. D 46 (1992) 1973.
[17] M. Glück, E. Reya, A. Vogt, Phys. Rev. D 45 (1992) 3986.
[18] S. Frixione, M.L. Mangano, P. Nason, G. Ridolfi, Nucl. Phys. B 412 (1994) 225, arXiv:hep-ph/9306337.
[19] B.A. Kniehl, G. Kramer, I. Schienbein, H. Spiesberger, Phys. Rev. D 77 (2008) 014011, arXiv:0705.4392 [hep-ph].
[20] H.L. Lai, M. Guzzi, J. Huston, Z. Li, P.M. Nadolsky, J. Pumplin, C.-P. Yuan, Phys. Rev. D 82 (2010) 074024, arXiv:1007.2241 [hep-ph].
[21] S. Alekhin, et al., Eur. Phys. J. C 75 (2015) 304, arXiv:1410.4412 [hep-ph], https://wiki-zeuthen.desy.de/HERAFitter.